

296

**NUMERICAL CALCULATIONS OF
ION SCATTERING IN SOLIDS**

by

K.K. Kwok

PART A: MCMASTER (ON-CAMPUS) PROJECT*

A project* report submitted in partial fulfillment of
the requirements for the degree of
Master of Engineering

Department of Engineering Physics

McMaster University

Hamilton, Ontario, Canada

April, 1975

* One of two project reports. The other one is designated PART B:
OFF-CAMPUS PROJECT.

K.K. Kwok

McMaster University
Hamilton, Ontario

TITLE: NUMERICAL CALCULATIONS OF ION SCATTERING
IN SOLIDS

SUPERVISOR: Dr. J.E. Robinson, Department of Engineering
Physics, McMaster University, Hamilton,
Ontario

NUMBER OF PAGES: 36

CONTENTS

	<u>Page</u>
ABSTRACT	i
ACKNOWLEDGEMENTS	ii
LIST OF FIGURES	iii
GLOSSARY OF SYMBOLS	iv
1. INTRODUCTION	1
2. GENERAL THEORY	3
2.1 Ion Penetration in Amorphous Solids	3
2.1.1 Electronic Stopping	3
2.1.2 Nuclear Stopping	5
2.2 Channeling	5
2.2.1 Continuum Potentials	6
2.2.2 Critical Angles	8
2.3 Dechanneling	9
3. COMPUTATION TECHNIQUE	11
4. COMPUTATIONS AND RESULTS	14
5. CONCLUSIONS	21
APPENDIX	22
REFERENCES	36

ABSTRACT

The motion of energetic charged particles inside a crystalline solid is strongly dependent upon the orientation of the ion beam and target. This effect is commonly known as the "channeling" effect. In this report, the development of a computer code is presented which simulates the 3-D ion scatterings experienced by energetic particles moving in a crystalline solid. A Monte Carlo technique is incorporated in the code to calculate scattering angles, range distribution, backscattering distribution and angular distribution of incident ions. The Thomas-Fermi interatomic potential is used for binary collision process and the continuum potential is used for the potentials experienced by the channeled ions inside crystal lattices.

ACKNOWLEDGEMENTS

I would like to thank deeply:

My supervisor, Dr. J.E. Robinson for his supervision,
discussions, helpful advices and encouragements
throughout the course of this work.

National Research Council of Canada, Ottawa, for an
award of a scholarship.

LIST OF FIGURES

	<u>Page</u>
FIGURE 1.1 CHANNELING	1
FIGURE 1.2 SCHEMATIC OF PROJECTED RANGE FOR AMORPHOUS TARGETS	2
FIGURE 1.3 SCHEMATIC OF PROJECTED RANGE FOR CRYSTALLINE TARGETS	2
FIGURE 2.1 CRITICAL ANGLE FOR CHANNELING	6
FIGURE 2.2 CONTINUUM POTENTIAL MODEL	7
FIGURE 4.1 CALCULATED PENETRATION DEPTH OF A CHANNELED ION VERSUS INCIDENT ENERGY ($E_0 = 1.2$ Kev)	15
FIGURE 4.2 CALCULATED PENETRATION DEPTH OF A CHANNELED ION VERSUS INCIDENT ENERGY ($E_0 = 4.6$ Kev)	15
FIGURE 4.3 CALCULATED PENETRATION DEPTH OF A CHANNELED ION VERSUS INCIDENT ENERGY ($E_0 = 20$ Kev)	16
FIGURE 4.4 RANGE DISTRIBUTION OF (H^+ , Si) AT IN- CIDENT ENERGY OF 1.2 Kev (CRYSTALLINE CASE)	17
FIGURE 4.5 RANGE DISTRIBUTION OF (H^+ , Si) AT IN- CIDENT ENERGY OF 1.2 Kev (AMORPHOUS CASE)	18
FIGURE 4.6 RANGE DISTRIBUTION OF (He, Si) AT IN- CIDENT ENERGY OF 2.7 Kev (CRYSTALLINE CASE)	19
FIGURE 4.7 RANGE DISTRIBUTION OF (He, Si) AT IN- CIDENT ENERGY OF 2.7 Kev (AMORPHOUS CASE)	20

GLOSSARY OF SYMBOLS

<u>Symbol</u>	<u>Description</u>
a	Thomas-Fermi screening radius
a_0	Bohr radius = 0.529 Å
A_1	Atomic mass number of incident ion
A_2	Atomic mass number of target ion
d	Distance between atoms in a row
d_p	Interplanar distance
e	Electronic charge
m_e	Electron rest mass
N	Atomic density
N_T	Total number of incident ions
N_B	Numbers of backscattered ion
N_C	Numbers of channeled ion
ρ_{ax}	Axial rms vibrational amplitude
v	Incident ion velocity
v_0	Bohr velocity = 2.2×10^8 cm/sec.
\hat{E}	Transverse energy
$\hat{\epsilon}$	Reduced transverse energy
$\hat{\epsilon}^*$	Critical transverse energy
T	Absolute temperature; Energy transferred
$V(r)$	Interatomic potential
ψ_1	Characteristic angle for axial channeling (high energy case)
ψ_2	Characteristic angle for axial channeling (low energy case)

1. INTRODUCTION

When an energetic ion strikes a solid target, many possible physical phenomena, such as Rutherford scattering, secondary electron emission, sputtering, X-ray production, energy-loss processes etc., can occur. If the target material is homogeneous and isotropic and has a random lattice structure, then the yields of these phenomena are not strongly orientation dependent. However, when the target material is monocrystalline, there is a probability for the incident to traverse along the open spaces between atomic rows or planes and to be steered by a correlated series of gentle small angle collision provided by the crystal lattices. Figure 1.1 shows schematically this effect.

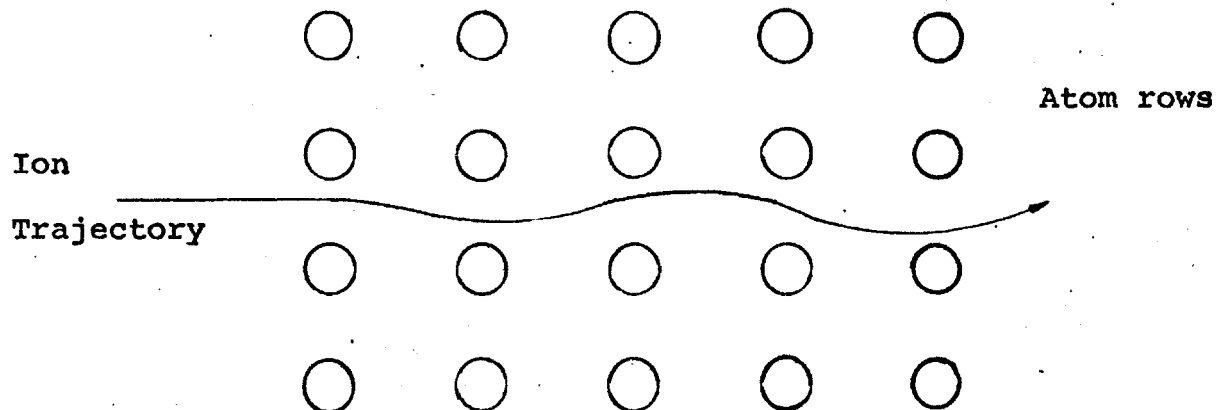


FIGURE 1.1 - CHANNELING

This effect is commonly known as the channeling effect. Figures 1.2 and 1.3 illustrate typical range distributions in amorphous targets and crystalline targets respectively. The suppression of nuclear loss accounts for the long penetrating 'tail' as shown in Figure 1.3.

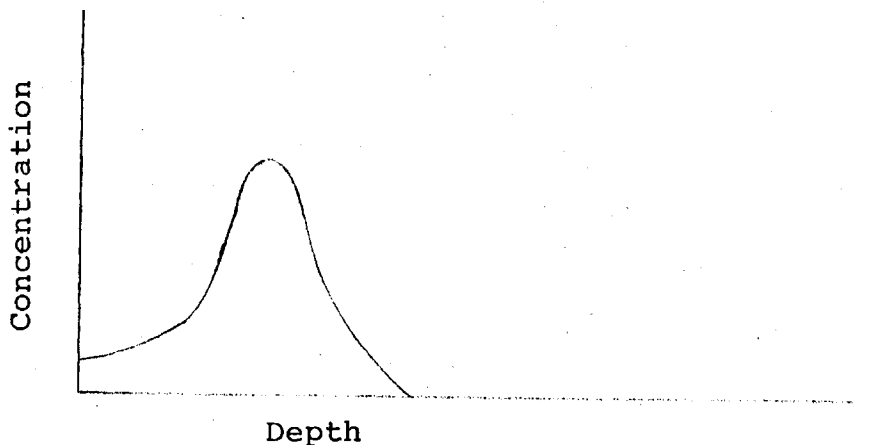


FIGURE 1.2 - SCHEMATIC OF PROJECTED RANGE FOR
AMORPHOUS TARGETS

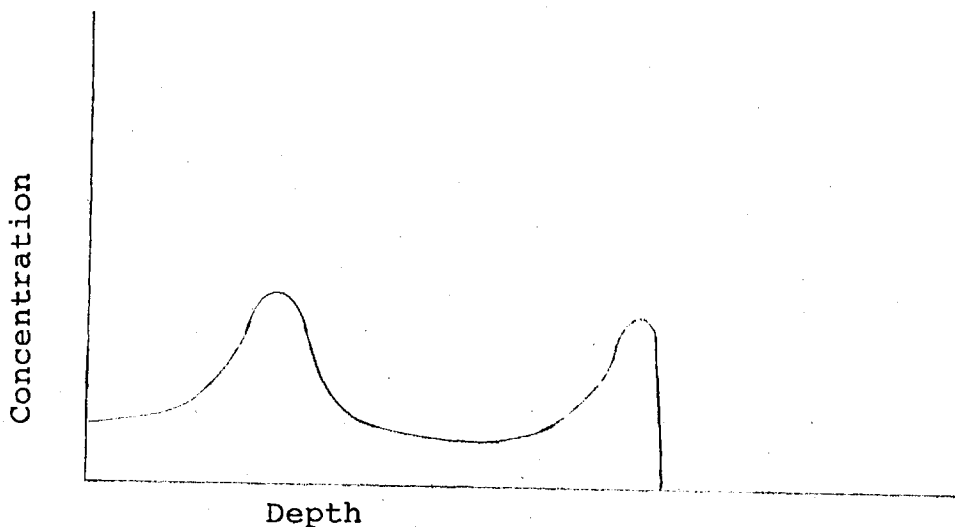


FIGURE 1.3 - SCHEMATIC OF PROJECTED RANGE FOR
CRYSTALLINE TARGETS

2. GENERAL THEORY

2.1 Ion Penetration in Amorphous Solids

For an amorphous solid in which the directional effect of the crystal lattice can be ignored, the range distribution is approximately gaussian in shape (see Figure 2.1) and can be characterized by a mean range and a straggling about this mean range. An understanding of the range profile of the implanted ion requires a detailed knowledge of the energy loss processes that slow down the traversing ion in the solid. In this calculation, the energy loss of the incident ion in the target consists of two independent categories of energy loss mechanisms.

- (1) Nuclear stopping - kinetic energy of the incident particle is transmitted to the target atom due to collisions. This is usually refer to as elastic scattering since the total energy of the ion-target pair is conserved and the interaction between incident and target atoms causes scattering of the incident ion.
- (2) Electronic stopping - energy loss as a result of the interaction of the ion with the electrons in the target atoms.

Each of these energy loss mechanisms will be taken up in greater details in subsequent sections.

2.1.1 Electronic Stopping

Based on LSS's theoretical treatment, at low energy, where the stopping power is proportional to ion

velocity, electronic stopping is assumed to be of the form [1,2] :

$$\frac{dE}{dx} = - K E^{1/2} \quad (2.1)$$

where K is given by

$$K = z_1^{1/6} \frac{z_1 z_2}{(z_1^{2/3} + z_2^{2/3})^{3/2}} \frac{8\pi N e^2 a_0 (\frac{1}{E'})^{1/2}}{} \quad (2.2)$$

Where N is the number of target atoms per unit volume, a_0 is the Bohr radius, E' is the energy at which the ion velocity equals the velocity of an electron in the first Bohr orbit, E is the ion energy, $z_1 (z_2)$ is the atomic number of the projectile (target) and e is electronic charge. It is convenient to express the above equation in terms of dimensionless parameters ρ and ϵ so that equation (2.1) becomes

$$\frac{d\epsilon}{d\rho} = - \kappa \epsilon^{1/2} \quad (2.3)$$

where $\rho = RNM_2^2 \pi a^2 \frac{4 M_1}{(M_1 + M_2)^2}$ (2.4)

$$\epsilon = \frac{EaM_2}{z_1 z_2 e^2 (M_1 + M_2)} \quad (2.5)$$

M_1, M_2 being the masses of the projectile and target respectively, R is distance and a is the Thomas-Fermi screening length and κ is defined as

$$\kappa = \xi_e \frac{0.0793 z_1^{1/2} z_2^{1/2} (A_1 + A_2)^{3/2}}{(z_1^{2/3} + z_2^{2/3})^{3/4} A_1^{3/2} A_2^{1/2}} \quad (2.6)$$

$$\xi_e \approx z_1^{1/6}$$

2.1.2 Nuclear Stopping

Nuclear stopping is obtained by solving numerically the Thomas-Fermi equation where the differential cross section of energy transfer is given by [3],

$$d\sigma = \pi a^2 \frac{dt}{2t^{3/2}} f(t^{1/2}) \quad (2.7)$$

where $t^{1/2} = \epsilon \sin(\theta/2)$ and θ is the scattering angle in COM (centre of mass) system, a is given by

$$a = 0.468(z_1^{2/3} + z_2^{2/3})^{-1/2} \quad (2.8)$$

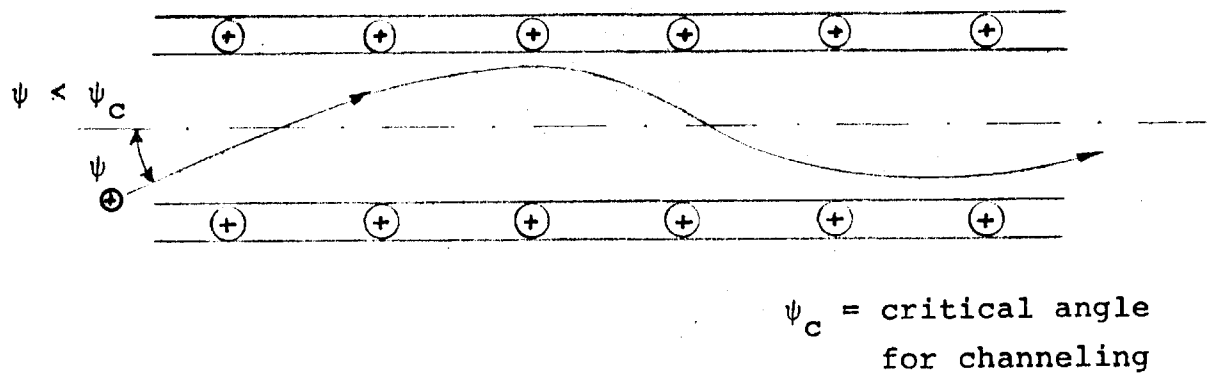
and $f(t^{1/2})$ is approximated by the expression

$$f(t^{1/2}) = 1.309 t^{1/6} [1 + (2.618t^{2/3})^{2/3}]^{-3/2} \quad (2.9)$$

2.2 Channeling

When an ion is incident on a solid in a direction close to the direction of an open channel and at an angle smaller than the critical angle, it will undergo a series of correlated small angle collision with the lattice atoms.

A repulsive force is provided by the lattice atoms, causing the ion to move across the centre of the channel to the opposite channel wall. Figure 2.1 illustrates the influence of the lattice atoms on a channeled ion and the critical angle for channeling.



ψ_c = critical angle
for channeling

FIGURE 2.1 - CRITICAL ANGLE FOR CHANNELING

Consequently nuclear stopping is suppressed and electronic stopping dominates. The ion can then penetrate more deeply into the target.

2.2.1 Continuum Potentials

The continuum model was first presented by Lindhard [4] to describe the interaction potentials between channelled particles and atomic rows or planes. In this model, the periodic potential of an atom row or plane is replaced by a potential averaged over a direction parallel to a row or

plane so that the potential due to a string of atoms is uniformly smeared out along the row. Therefore, it is possible to describe the motion of an ion in the plane transverse to the string or in the line transverse to the plane as in the planar case.

The continuum potential depends only on the distance ρ from the row (or plane) and not on the position z along it. This implies conservation of momentum in the z direction and the trajectory of the ion can be described completely in a plane transverse to the string. For an isolated row, the expression for static and planar potentials are

$$V_{AS}(\rho) = \frac{1}{d} \int_{-\infty}^{\infty} V[(\rho^2 + z^2)^{1/2}] dz \quad (2.10)$$

$$V_{PS}(\rho) = n \int_0^{\infty} 2\pi R V[(\rho^2 + R^2)^{1/2}] dR \quad (2.11)$$

where d is the distance between atoms in a row and n is the areal density of atoms in the plane.

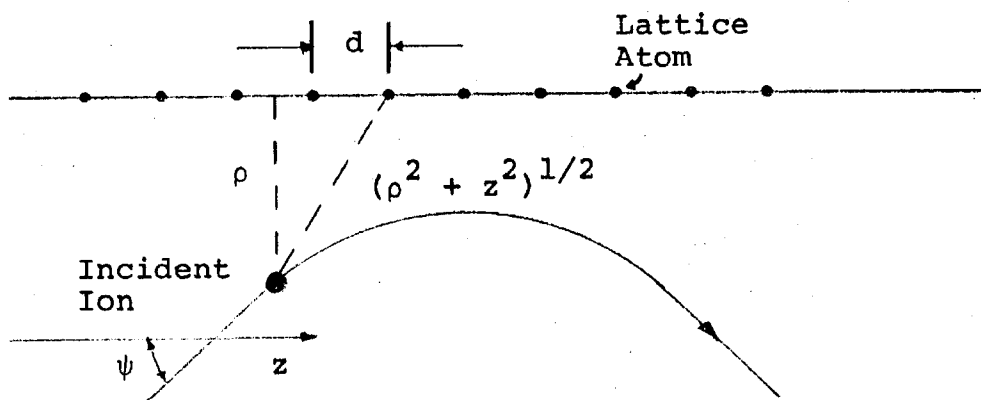


FIGURE 2.2 - CONTINUUM POTENTIAL MODEL

2.2.2 Critical Angles

The condition for the validity of the continuum model is when the ions remain relatively far from the atomic strings with a low transverse angle to them. The continuum approximation breaks down when the ion enters at an angle larger than the critical angle or when the ion has gained sufficient transverse energy to penetrate into the core of the string of atoms by overcoming the potential barrier and thus becomes scattered as in the amorphous case.

The critical angle used by Lindhard is referred to as the maximum angle at which a trajectory could be incident on a row or plane of atoms and deflected by the row or plane to sustain a stable trajectory. It was found that at high energy condition, i.e. $E > E'$ where E' is given by

$$E' = 2Z_1 Z_2 e^2 / d \quad (2.12)$$

the criteria for stable trajectory is

$$\psi < \psi_1 = 2(Z_1 Z_2 e^2 / (Ed))^{1/2} \quad (2.13)$$

At low energy condition, $E < E'$,

$$\psi < \psi_2 = 1.5^{1/4} (a \psi_1 / d)^{1/2} \quad (2.14)$$

where ψ_1 and ψ_2 are applicable with $E = E'$

In the planar case $\psi_1 = 0.93\psi_a$

where $\psi_a = (2\pi Z_1 Z_2 e^2 a N d_p / E)^{1/2}$ (2.15)

and d_p is the planar distance.

2.3

Dechanneling

In the continuum model, the transverse energy of a channeled ion is considered to be constant. However, when the thermal vibrations of the lattice atoms are taken into consideration, the transverse energy, \hat{E} , of the ion changes with time due to interactions both with the electrons in the solid and the vibrating lattice atoms. The transverse energy may becomes larger than the critical value for stable channeling. The expression for the average rate of increase of the transverse energy due to the vibrating lattice is [5],

$$\frac{d}{dz} \langle \hat{E} \rangle_n = \frac{\pi N d^2 \rho_{ax}^2}{E_0 C^2 a^2} \left(\frac{z_1 z_2 e^2}{d} \right)^2 \frac{A \exp(\hat{\epsilon}) - 1}{A (\exp(\hat{\epsilon}) - 1)} \\ \left(A \exp(\hat{\epsilon}) + \frac{3}{2} \right) \left(1 - \frac{\exp(-\hat{\epsilon})}{A} \right)^3 \quad (2.16)$$

and the expression for \hat{E} due to electronic collisions is

$$\frac{d}{dz} \langle \hat{E} \rangle_e = \frac{2 m_e v^3 N d \xi_e \pi a_0}{E_0 v_0} \left(\frac{z_1 z_2 e^2}{d} \right)^2 \left(\frac{z_2}{z} \right) \frac{A \exp(\hat{\epsilon}) - 1}{A (\exp(\hat{\epsilon}) - 1)} \\ \left[\frac{\exp(-\hat{\epsilon})}{A} \right] \left(1 - \frac{\exp(-\hat{\epsilon})}{A} \right) \quad (2.17)$$

where

$$c^2 = 3$$

$$A = \frac{c^2 a^2}{r_o^2} + 1 \quad (2.18)$$

$$r_o^2 = (Nd\pi)^{-1} \quad (2.19)$$

$$z = (z_1^{2/3} + z_2^{2/3})^{3/2} \quad (2.20)$$

3. COMPUTATION TECHNIQUE

The main features of this computer code are:

(1) The Monte Carlo technique incorporated in the calculation uses 3 random numbers at each collision to determine the direction (i.e. the scattering angles), energy of the emerging ion and the distance between collisions. A random number q_1 is used to determine the location of nuclear scattering [6,7]. A second random number q_2 is used to find the scattering angle in COM system. The energy transferred and the scattering angle is related by

$$\frac{T}{T_m} = \sin^2 (\theta/2) \quad (3.1)$$

where $T_m = \gamma E_0$. (3.2)

$$\gamma = 4M_1 M_2 / (M_1 + M_2)^2 \quad (3.3)$$

The azimuthal angle ϕ is determined by the third random number q_3 so that ϕ is given by

$$\phi = 2\pi q_3 \quad (3.4)$$

For a given initial energy E_0 we determine the first nuclear collision location (i.e. the distance between collision and the scattering angles), energy after collision, energy transferred and the projected range. Once the first location has been determined, further random

numbers are generated to find the second collision location. It can be shown [8] that for subsequent collisions the new scattering angles after $n+1$ collisions in the laboratory system are given by

$$\cos(\theta_{n+1}) = \cos\theta_n \cos\theta_1 - \sin\theta_n \cos\phi_1 \sin\theta_1 \quad (3.5)$$

$$\begin{aligned} \sin(\phi_{n+1}) &= (\cos\theta_n \sin\phi_n \cos\phi_1 \sin\theta_1 + \cos\phi_n \sin\phi_1 \sin\theta_1 \\ &\quad + \sin\theta_n \sin\phi_n \cos\theta_1) / \sin\theta_{n+1} \end{aligned} \quad (3.6)$$

The projected range is

$$P = \sum^n (\text{actual distance})_n \cos(\theta_{n+1}) \quad (3.7)$$

(2) A check is made at each collision to determine (i) whether the projected range is negative or positive. In the former case the ion is considered to be backscattered. (ii) whether the ion falls within a channel direction. If so, the ion is considered to be channeled. The range of a channeled ion is evaluated as the followings.

Equations (2.16) and (2.17) can be put into the following forms,

$$\frac{d}{dz} \langle \hat{\epsilon} \rangle_n = A_n(E_0, T) f_n(\hat{\epsilon}) \quad (3.8)$$

$$\frac{d}{dz} \langle \hat{\epsilon} \rangle_e = B_e(E_0, T) f_e(\hat{\epsilon}) \quad (3.9)$$

where $f_n(\hat{\epsilon}) = \frac{A \exp(\hat{\epsilon}) - 1}{A(\exp(\hat{\epsilon}) - 1)} (A \exp(\hat{\epsilon}) + \frac{2}{3})(1 - \exp(-\hat{\epsilon})/A)^3 \quad (3.10)$

$$f_e(\hat{\epsilon}) = \frac{A \exp(\hat{\epsilon}) - 1}{A(\exp(\hat{\epsilon}) - 1)} (1 - \exp(-\hat{\epsilon})/A) \left(\frac{\exp(-\hat{\epsilon})}{A} \right) \quad (3.11)$$

For a given temperature and incident energy, equations (3.8) and (3.9) becomes

$$\frac{d}{dz} \langle \hat{\epsilon} \rangle_n = A_n f_n(\hat{\epsilon}) \quad (3.12)$$

$$\frac{d}{dz} \langle \hat{\epsilon} \rangle_e = B_n f_e(\hat{\epsilon}) \quad (3.13)$$

Addition of equations (3.12) and (3.13) yields the total rate of increase of the transverse energy $\langle \hat{\epsilon} \rangle$. Therefore,

$$\frac{d}{dz} \langle \hat{\epsilon} \rangle = A_n f_n(\hat{\epsilon}) + B_n f_e(\hat{\epsilon}) \quad (3.14)$$

Equation (3.14) can be solved numerically on a computer to give the penetration depth. The ion is considered to be dechanneled when the transverse energy exceeds the critical value, i.e. when $\hat{\epsilon} > \hat{\epsilon}^*$, where $\hat{\epsilon}^*$ is given by

$$\hat{\epsilon}^* = \frac{Ca}{(2^{3/2}\psi_1)d} \quad (3.15)$$

The procedure is continued until the ion history is terminated.

4. COMPUTATIONS AND RESULTS

Two computer programs have been developed; one for the amorphous case and the other is essentially the same except for the consideration of the directional effect. The former was used for comparison purposes. In the latter, the crystalline solid is assumed to have a diamond structure with seven open channels. When an energetic, positively charged ion starts to make its way into the solid, its orientation is determined by the steps as described in Section 3. If the orientation of the incident ion does not lie in a channeled direction, the ion is considered to be scattered as in amorphous case. However, if in the meantime, the ion is scattered into a channeled direction, the ion is considered to be channeled. This phenomena - quasi-channeling - describes the transition from a random trajectory to a channeled one. All energy loss processes and depth penetration are calculated corresponding to those as described in Sections 2.2 and 3. The channeled ion may subsequently either be dechanneled and if upon emerging from the channel, the ion still possesses sufficient energy, it is considered to be scattered continuously as before until the ion history is terminated, or be stopped inside the channel. In both cases the ion history is considered to be terminated if the energy of the ion is less than 25 ev.

To test the code, trajectories of (H^+, Si) at incident energy of 1.2 Kev and (He, Si) at an incident energy of 2.7 Kev were traced for 300 particles. Typical results of the projected ranges in both cases are shown in Figures 4.4 through 4.7. Comparisons of the projected ranges in the amorphous cases with the crystalline cases showed that deeper penetrations were recorded. Also, in both cases, backscattering yields were reduced in the crystalline case.

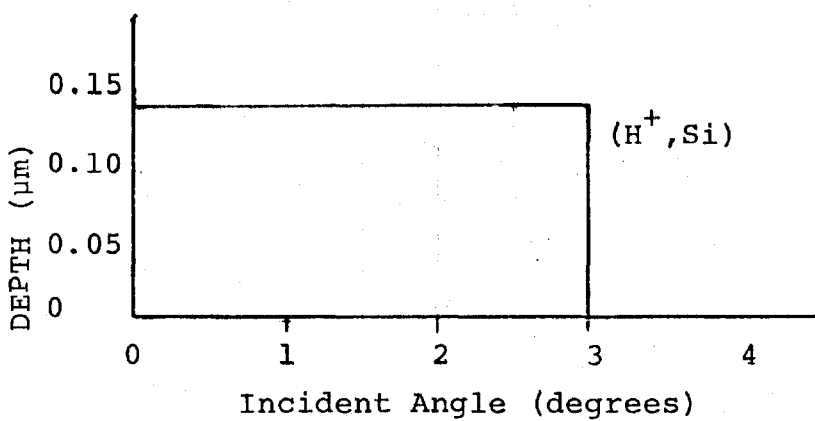


FIGURE 4.1 - CALCULATED PENETRATION DEPTH OF
A CHANNELLED ION VERSUS INCIDENT ANGLE
($E_0=1.2$ Kev)

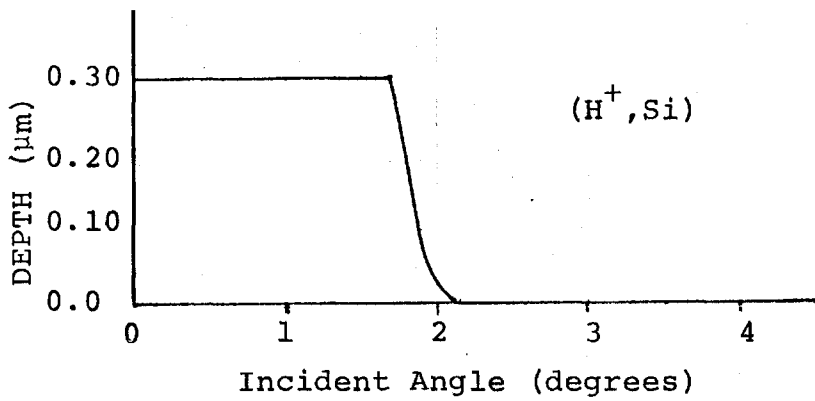


FIGURE 4.2 - CALCULATED PENETRATION DEPTH OF
A CHANNELLED ION VERSUS INCIDENT ANGLE
($E_0=4.6$ Kev)

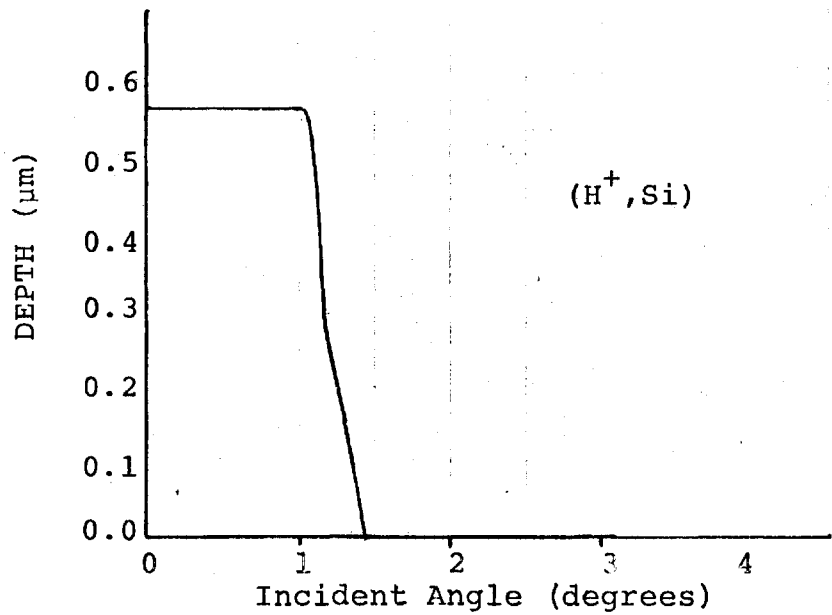


FIGURE 4.3 - CALCULATED PENETRATION DEPTH OF
A CHANNELLED ION VERSUS INCIDENT ANGLE
($E_0 = 20$ Kev)

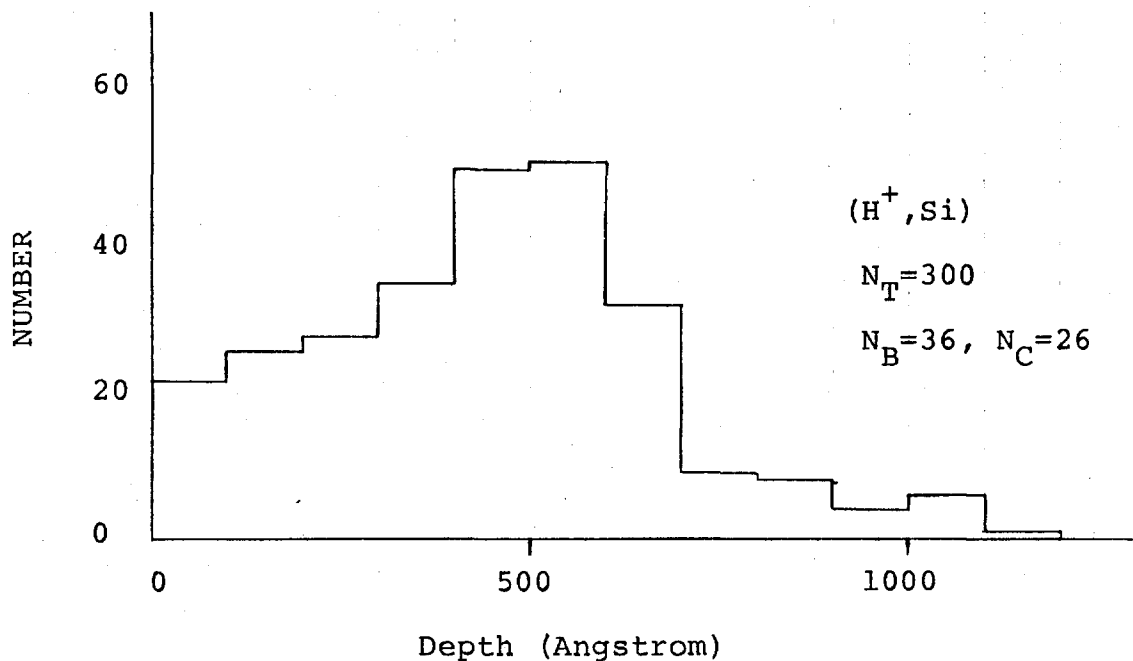


FIGURE 4.4 - RANGE DISTRIBUTION OF (H^+, Si) AT
INCIDENT ENERGY OF 1.2 Kev
(CRYSTALLINE CASE)

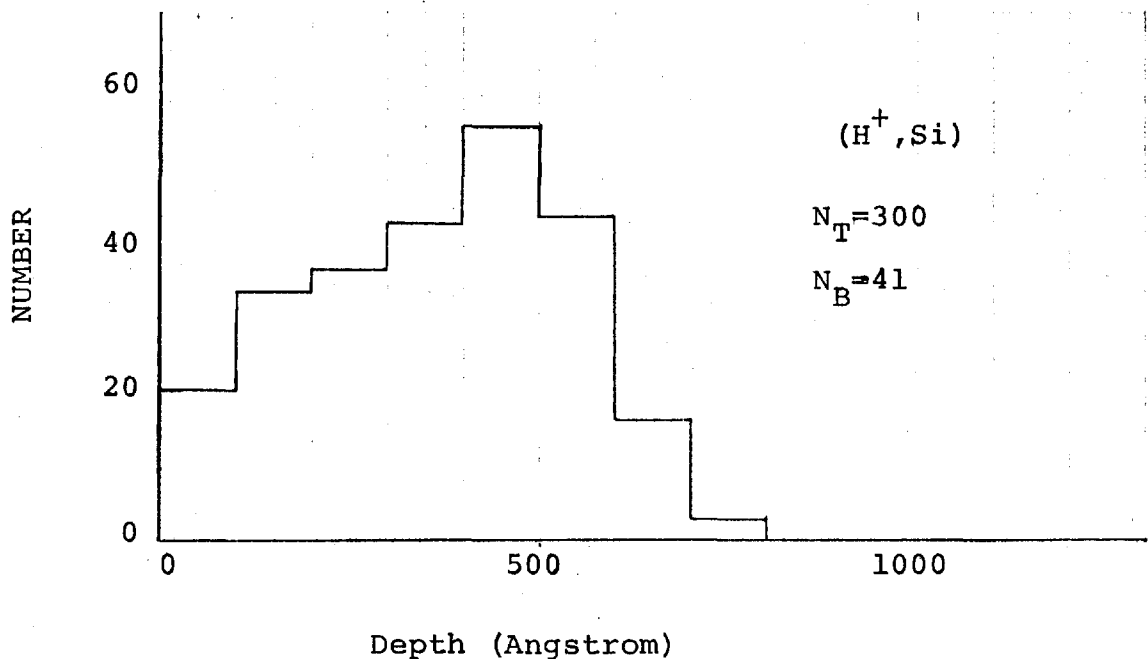


FIGURE 4.5 - RANGE DISTRIBUTION OF (H^+, Si) AT
INCIDENT ENERGY OF 1.2 Kev
(AMORPHOUS CASE)

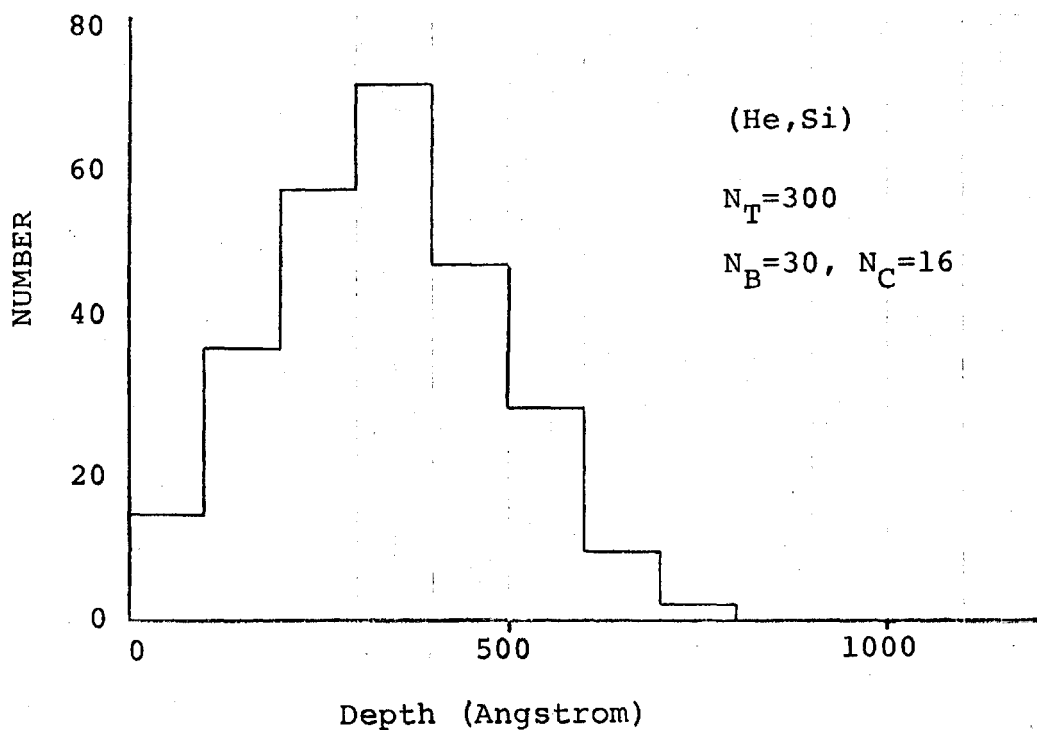


FIGURE 4.6 - RANGE DISTRIBUTION OF (He, Si) AT
INCIDENT ENERGY OF 2.7 Kev
(CRYSTALLINE CASE)

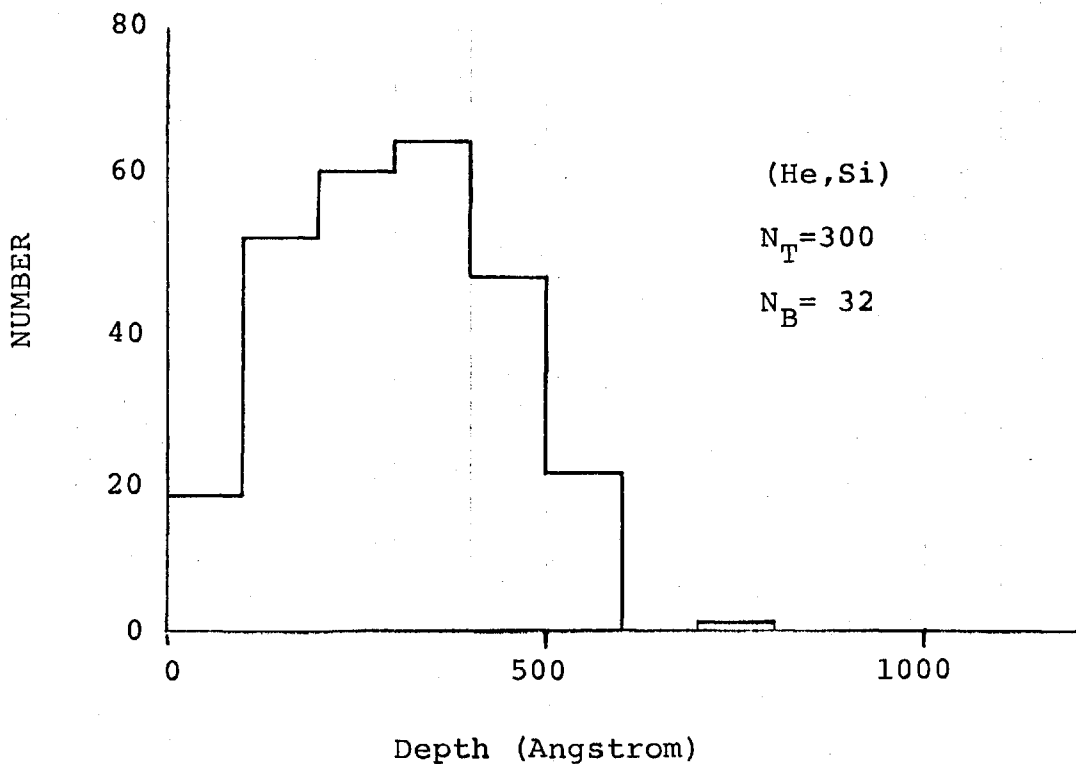


FIGURE 4.7 - RANGE DISTRIBUTION OF (He, Si) AT
INCIDENT ENERGY OF 2.7 Kev
(AMORPHOUS CASE)

5. CONCLUSIONS

A computer code, incorporating a Monte Carlo technique and the directional effect of crystalline solids has been developed to investigate the dechanneling of energetic ions in crystalline solids and hence to calculate the projected range. The code was tested using H incident on Si and He incident on Si. Comparisons of results with those obtained using an amorphous code showed that penetration depths were enhanced and backscattering yields were reduced as well. The results obtained were reasonable and satisfied the objective of this study.

APPENDIX

GUSP,T777.

DISPOSE,OUTPUT,*P2.

FTN,T,OPT=2.

ATTACH,TAPE1,XMATRIX,ID=GUSH,CY=2.

LGO.

6400 END OF RECORD

PROGRAM TST (INPUT,OUTPUT,TAPE5=INPUT,TAPE6=OUTPUT,TAPE1)

C ATOMIC SCATTERING AND TRANSPORT CODE

C USING THOMAS-FERMI INTERACTION POTENTIAL

C CONSIDERING BOTH ELECTRONIC AND NUCLEAR SCATTERING

EXTERNAL FE,FN,FTT

COMMON B,CE,CN

INTEGER FREQ

DIMENSION ENDIST(50)

DIMENSION FD030(50),FD3060(50),FD6090(50)

DIMENSION R(40),F(40),EPSI(2),D(2),

1 PRPP(350), ECOLT(50),ETOTA(50),ECOLE(50),ECOLA(50),

1THET(209,19),F(209),EPSARR(19)

DIMENSION PHI(2)

DATA ENDIST/50*0./

DATA FD030/50*0./,FD3060/50*0./,FD6090/50*0./

DATA PRPP/350*0./,ECOLT/50*0./,ETOTA/50*0./,ECOLE/50*0./

*,ECOLA/50*0./

C INPUT CONSISTS OF EPSAAR ,THE REDUCED ENERGY

DATA (EPSARR(1),I=1,19)/.1,.2,.3,.4,.5,.6,.7,.8,.9,

* .1,.2,.3,.4,.5,.6,.7,.8,.9,.10./

C F, A UNIFORMLY DISTRIBUTED NO.BETWEEN ZERO AND ONE

NFPS=19

C GENERATE F

DO 28 I=1,199

28 F(I)=I*.005

DO 10 I=1,10

10 F(I+199)=.995+I*.0005

F(NF)=1.0

C THET IS THE SCATTERING ANGLE IN THE C.O.M. SYSTEM AND

C THE MASS AND ATOMIC NOS. OF THE TARGET MATERIAL AND THE

C INCIDENT IONS ARE DENOTED BY A2,A1,Z2,AND Z1.

C RHO IS THE DENSITY OF THE TARGET MATERIAL.

REWIND 1

READ(1) ((THET(I,J),J=1,NEPS),I=1,NF)

IF(FOF(1))100,555

100 STOP 100

555 READ(5,1) A1,A2,Z1,Z2,RHO

READ (5,94) RHOAX

READ (5,94) T

READ (5,93) NP

WRITE (6,94) RHOAX

WRITE (6,94) T

WRITE (6,93) NP

C ET IS THE INITIAL ENERGY OF THE INCIDENT IONS

DATA PI,ET,M,FBKT,ANGT/3.14159265,0.5,0,0.,0./

FI=1.2

DENOM=(Z1**(2./2.)+Z2**(2./2.))**(1./2.)

C SR IS THE SCREENING RADIUS

SR=0.8853*0.529*.1E-07/DENOM

C EPS=C*F

C=A2/(A1+A2)*SR/(Z1*Z2*(4.8*.1E-09)**2)

CON22=1.6021*.1E-08

CON603=C*CON22
CON124=2.* (CON22)**.5
C AV IS AVOGADROS NUMBER
C AD IS ATOMIC DENSITY OF TARGET MATERIAL
AV=0.602252*.1E+25
AD=RHO*AV/A2
C (DE/DX) FOR ELECTRONIC ENERGY LOSS=EK*E**0.5
EK=8.*PI*AD*(4.8*.1E-09)**2*.529*.1E-07/(25.*1.6021*.1E-08)**0.5*
Z1**(.7/.6.)*Z2/(DENOM)**3
A=A2/A1
ALPHA=((A-1.)/(A+1.))**2
READ(5,4) (R(I),I=1,40),(E(I),I=1,40)
WRITE(6,3)
WRITE(6,2) EI
WRITE(6,3)
WRITE(6,1) A1,A2,Z1,Z2,RHO
WRITE(6,6) A1
WRITE(6,6) A2
WRITE(6,6) Z1
WRITE(6,6) Z2
WRITE(6,6) RHO
Y=2.*(EI*1.6021*1.E-09)**.5/EK
WRITE(6,20) EK
WRITE(6,20) Y
ZMAX=Y
MM=0
G=3.***0.5
Z=(Z1**(.2/.3.)+Z2**(.2/.3.))**(.3/.2.)
AT=0.4685*1.E-08*Z**(-1./3.)
RO=(AD*T*PI)**(1./2.)
PHI1=(2.*Z1*Z2*(4.8*0.1E-09)**2/(EI*1.6021*.1E-08*T))**0.5
B=3.*AT**2/(RO**2)+1.0
V=(2.*EI*1.6021*.1E-08/A1)**0.5
PHIC=(G*AT/(2.***0.5*T)*PHI1)**0.5
AME=9.11*1.E-28
VO=2.2*1.0E+08
AO=0.528*1.E-08
ETA=Z1**1./6.
CN1=(PI*AD*T**2)/(EI*1.6021*1.0E-09*G**2*AT**2)
CN2=(Z1*Z2*(4.8*.1E-09)**2/T)
CN=CN1*CN2*RHOAX**2
CE1=2.*AME*AD*T*ETA*PI*AO/(EI*1.6021*1.0E-09*VO)
CE2=Z2/Z
CE3=V**3
CE=CE1*CE2*CN2*CE3
EC=G*AT/(2.***1.5*T*PHI1)

WRITE(6,5)
WRITE(6,3)
EMIN=EI
EMAX=0.
DO 400 N=1,300
WRITE(6,922) N
NN=0
EI=1.2
K=1
ANGL=0.
EPSI(1)=0.

EPSI(2)=0.
PHI(1)=0.
PHI(2)=0.
PR1=0.
DETA=0.
FHI=0.
PRX1=0.
PRY1=0.
PRZ1=0.
C EPSI SCATTERING ANGLE IN LAB SYSTEM IN RADS
C PHI AZIMUTHAL ANGLE
C PR PROJECTED RANGE
500 IF(EI-E(8)) 705,705,706
706 IF(EI-E(16)) 707,707,708
708 IF(EI-E(24)) 709,709,710
710 IF(EI-E(32)) 711,711,712
712 NA=32
NR=40
GO TO 750
705 NA=1
NB=8
GO TO 750
707 NA=8
NB=16
GO TO 750
709 NA=16
NB=24
GO TO 750
711 NA=24
NB=32
750 DO 800 I=NA,NB.
IF(EI-F(I)) 802,801,800
800 CONTINUE
801 EI=F(I)
R0=R(I)
GO TO 803
802 R0=R(I-1)+(R(I)-R(I-1))/(E(I)-E(I-1))*(EI-E(I-1))
803 CALL FRANDN (RN1,1,0)
IF(RN1.EQ.1.) GO TO 400
DFLR=ALOG(1.-RN1)
R1=R0+DFLR
IF (R1.LT.R(1)) GO TO 400
IF(R1-R(8)) 605,605,606
606 IF(R1-R(16)) 607,607,608
608 IF(R1-R(24)) 609,609,610
610 IF(R1-R(32)) 611,611,612
612 NA=32
NR=40
GO TO 911
605 NA=1
NB=8
GO TO 911
607 NA=8
NB=16
GO TO 911
609 NA=16
NB=24
GO TO 911

611 NA=24
NR=32
911 DO 600 I=NA,NB
IF(R1-R(I)) .EQ. 602,601,600
600 CONTINUE
601 R1=R(I)
ER=F(I)
GO TO 603
602 ER=E(I-1)+(E(I)-E(I-1))/(R(I)-R(I-1))*(R1-R(I-1))
603 EPS=CON603*ER
124 D(K)=CON124/EK*(SQRT(EI)-SQRT(ER))
IF(D(K).LT.5.E-08) D(K)=2.E-08
C D(K) IS ACTUAL DISTANCE TRAVERSED BY ION
AA=SIN(DFTA)*SIN(FHI)
BB=SIN(DFTA)*COS(FHI)
CC=COS(DFTA)
PX=D(K)*AA
PY=D(K)*BB
PZ=D(K)*CC
PRZ2=PRZ1+PZ
PRY2=PRY1+PY
PRX2=PRX1+PX
PRP=PRZ2*.1E+07
L=PRP
L=L+1
18 IF(PRZ2) 22,22,23
22 M=M+1
C BACK-SCATTERING ANGLE IS EPSI(1)
DS=-PRZ1/COS(EPSI(1))
DS=ARS(DS)
C DS IS THE DISTANCE TO THE SURFACE
ERK=(SQRT(EI*CON22)-.5*EK*DS)**2/CON22
ERKT=ERKT+ERK
C EPK BACK-SCATTERING ENERGY
BA=PI-EPSI(1)
BA1=PHI(1)
RA1=RA1*180./PI
RA=RA*180./PI
ANGT=ANGT+BA
C RA IS THE BACK-SCATTERING ANGLE IN DEGREES
WRITE(6,9) EBK,BA,BA1
L10=IFIX(ERK*10.)+1.
ENDIST(L10)=ENDIST(L10)+1.
IF (RA.LT.30.) FD030(L10)=FD030(L10)+1.
IF (RA.GE.30..AND.RA.LT.60.) FD3060(L10)=FD3060(L10)+1.
IF (RA.GE.60.) FD6090(L10)=FD6090(L10)+1.
IF (ERK.LT.EMIN) EMIN=ERK
IF (ERK.GT.EMAX) EMAX=ERK
WRITE(6,3)
WRITE(6,11) NN
WRITE(6,3)
GO TO 400
23 IF(ER.GT.0.10) GO TO 180
PRPP(L)=PRPP(L)+1.
GO TO 400
180 CALL FRANDN (PN2,I,0)
C CALCULATION OF SCATTERING ANGLE IN C.M. SYSTEM
IF (EPS-.1) 88,777,777

88 K1=1
GO TO 19
777 IF ((EPS-1.) .GT. 44,333,333
44 K1=IFIX(EPS*10.)
IF((EPS-EPSARR(K1)).GT..05) K1=K1+1
GO TO 19
333 K1=IFIX(EPS)+9
IF((EPS-EPSARR(K1)).GT..5) K1=K1 +1
19 IF(RN2-.005)89,90,90
89 K2=1
GO TO 919
90 IF (RN2.GE..95) GO TO 918
K2=IFIX(RN2*1000./5.)
GO TO 919
918 IF (RN2.GT..995) GO TO 917
K2=IFIX(RN2*1000./5.)
K3=K2+1
THETA1=THET(K2,K1)
THETA2=THET(K3,K1)
THETA=(THETA1+(RN2-F(K2)))*(THETA2-THETA1)/(F(K3)-F(K2))*PI/180.
GO TO 916
917 K2=IFIX((RN2-.995)/.0005)+199
K3=K2+1
THETA1=THET(K2,K1)
THETA2=THET(K3,K1)
THETA=(THETA1+(RN2-F(K2)))*(THETA2-THETA1)/(F(K3)-F(K2))*PI/180.
GO TO 916
919 THETA=THET(K2,K1)*PI/180.
916 FT=(SIN(THETA/2.))**2.
TVAR1=A*COS(THETA)
58 Q=(TVAR1 +1.)/(A**2+2.*TVAR1 +1.)**.5
EPSI(K)=ACOS(Q)
TVAR2=1.-ALPHA
93 FI=FB*(1.- TVAR2*FT)
C FT PARTICLE ENERGY AFTER NUCLEAR COLLISION.
Y=2.* (FI*1.6021*1.E-09)**.5/EK
FCOL=FB*TVAR2*FT
ECOLT(L)=ECOLT(L)+FCOL
IF(ECOL.GT.0.05) ECOLE(L)=ECOLE(L)+FCOL
172 NN=NN+1
IF(FI.GT.0.10) GO TO 170
PRPP(L)=PRPP(L)+1.
GO TO 400
170 CALL FRANDN (RN3,1,0)
PHI(K)=2.*PI*RN3
U1=EPSI(1)
U2=EPSI(2)
V1=PHI(1)
V2=PHI(2)
DETA=ACOS(COS(U1)*COS(U2)-SIN(U1)*COS(V2)*SIN(U2))
U11=SIN(U2)*SIN(V2)
U12=COS(U2)*SIN(U1)
U13=SIN(U2)*COS(V2)*COS(U1)
DFHI=ATAN(U11/(U12+U13))
FHI=DEHT+V1
IF (FHI.LT.0.) GO TO 60
GO TO 63
60 FHT=2.*PI+FHT

63 IF (FHI.GT.(2.*PI)) GO TO 61
GO TO 43
61 DO 66 I=1,20
X=FHI-I*2.*PI
IF (X.GT.(2.*PI)) GO TO 66
GO TO 65
66 CONTINUE
65 FHI=X
43 AA=SIN(DETA)*SIN(FHI)
BB=SIN(DETA)*COS(FHI)
CC=COS(DETA)
EPSTA=DETA*180./PI
PHTA=FHI*180./PI
152 IF (PHTA.LE. 2.. AND .PHTA.GE.358.) GO TO 51
IF (PHTA.LE. 2.. AND .PHTA.GE. 358.) GO TO 51
IF (EPSIA.LE. 2.. AND .EPSTA.GE. 358.) GO TO 53
IF (EPSIA.LE. 141.. AND . EPSIA.GE. 137.) GO TO 54
GO TO 80
54 IF (PHIA.LE. 47.. AND .PHIA.GE. 43.) GO TO 131
IF (PHIA.LE. 323.. AND .PHIA.GE. 313.) GO TO 132
IF (PHIA.LE. 92.. AND .PHIA.GE. 88.) GO TO 133
GO TO 80
53 IF (PHTA.LE. 137.. AND .PHTA.GE. 133.) GO TO 134
IF (PHTA.LE. 47.. AND .PHTA.GE. 43.) GO TO 135
GO TO 80
51 IF (EPSIA.LE. 2.. AND .EPSIA.GE. 358.) GO TO 136
IF (EPSIA.LE.47.. AND .EPSTA.GE.43.) GO TO 137
GO TO 80
131 FHD=ABS(EPSTA-139.0)*PI/180.
GO TO 140
132 FHD=ABS(EPSTA-139.0)*PI/180.
GO TO 140
133 FHD=ABS(EPSIA-139.0)*PI/180.
GO TO 140
134 IF(EPSIA.GE.358.) EPSIA=360.-EPSIA
FHD=ABS(EPSIA-0.)*PI/180.
GO TO 140
135 IF(EPSTA.GE.358.) EPSTA=360.-EPSTA
FHD=ABS(EPSTA-0.)*PI/180.
GO TO 140
136 IF(EPSIA.GE.358.) EPSIA=360.-EPSIA
FHD=ABS(EPSIA-0.)*PI/180.
GO TO 140
137 FHD=ABS(EPSTA-45.0)*PI/180.
GO TO 140
80 GO TO 36
140 WRITE (6,73)
WRITE (6,?)
MM=MM+1

C
C

IF (FHD.LE.0.026) GO TO 201
EP=FT*FHD**2*1.6021*1.E-09
FT=FP*(T/(Z1*Z2*(4.8*.1E-09)**2))
FRFO=10
DO 114 I=1,NP
W=ZMAX/NP
H=(I-1)*W

```
      WRITE(6,94) FT
      CALL RUNKUT(FTT,W,ET)
      IF (H.GT.Y) GO TO 201
      IF (FT.GT.FC) GO TO 116
114 CONTINUE
      GO TO 116
201 H=Y
      EI=0.05
116 AA=SIN(DETA)*SIN(FHI)
      BB=SIN(DETA)*COS(FHI)
      CC=ABS(COS(DETA))
      PX=AA*H
      PY=BB*H
      PZ=CC*H
      PRX2=PRX1+PX
      PRY2=PRY1+PY
      PRZ2=PRZ1+PZ
      WRITE(6,6) PZ
      PRINT(6,6) PRZ2
      PPP=PRZ2*.1E+07
      L=PPP
      L=L+1
      PRPP(L)=PRPP(L)+1.
36 EPSI(1)=DETA
142 PHI(1)=FHI
      PRZ1=PRZ2
      PRY1=PRY2
      PRX1=PRX2
      K=2
      GO TO 500
400 CONTINUE
      WRITE(6,7) M
      WRITE(6,3)
      WRITE(6,75) MM
      WRITE(6,3)
      RSN=M
      AFRK=FRKT/RSN
      WRITE(6,14) AFRK
      WRITE(6,3)
      AANG=ANGT/RSN
      WRITE(6,15) AANG
      WRITE(6,3)
      WRITE(6,13)
      WRITE(6,3)
      DO 900 L=1,350
      WRITE(6,12) PRPP(L)
.900  CONTINUE
      WRITE(6,3)
      TOTNP=10.
      EI=1.2
      TOTEN=TOTNP*EI
      WRITE(6,16)
      DO 910 L=1,50
      ETOTA(L)=ECOLT(L)/TOTEN
      WRITE(6,20) ETOTA(L)
.910  CONTINUE
      WRITE(6,3)
      WRITE(6,21)
```

```
DO 920 L=1,50
ECOLA(L)=ECOLE(L)/TOTEN
WRITE(6,20) ECOLA(L)
920 CONTINUE
WRITE (6,3)
WRITE (6,1003)
1003 FORMAT (5X,*NO. OF PARTICLES PER ENERGY INCREMENT*)
WRITE (6,3)
WRITE (6,3000)
3000 FORMAT (5X,*ENERGY INTERVALS*, 5X,*NO . OF PARTICLES*/12X,* (EV)*)
DO 1000 I=1,50
J10=I*100
J20=J10-100
PRINT 1001, J20,J10,ENDIST(I)
1000 CONTINUE
1001 FORMAT(7X,I4,*-* ,I4,12X,F10.4)
WRITE (6,3).
WRITE (6,3001)
3001 FORMAT (5X,*CLASSIFICATION OF BACK-SCATTERED PARTICLES ACCORDING*/
15X,*TO THE BACK-SCATTERED ENERGY AND THE BACK-SCATTERING ANGLE.*)
WRITE (6,3)
WRITE (6,3002)
3002 FORMAT (5X,*ENERGY INTRVALS*,5X,*NO. OF PARTICLES*,5X,*NO. OF PART
ICLES *,5X,*NO. OF PARTICLES*/11X,* (EV)*,16X,*0-30*,17X,*30-60*17X
1,*60-90*)
DO 3003 I=1,50
J20=J10-100
J10=I*100
WRITE (6,3004) J20,J10,ED030(I),ED3060(I),ED6090(I)
3003 CONTINUE
3004 FORMAT (7X,I4,*-* ,I4,10X;F10.4,11X,F10.4,12X,F10.4)
WRITE (6,3)
WRITE (6,1004) EMIN,EMAX
1004 FORMAT(5X,*MIN. BACKSCATTERED ENERGY=*,E15.7/5X,*MAX. BACK-SCATT
ERED ENERGY=*,E15.8)
1 FORMAT(2F10.7,2F4.1,F6.3)
2 FORMAT(5X,*INITIAL ENERGY=*,F5.2)
3 FORMAT(//)
4 FORMAT(E12.6)
5 FORMAT(5X,*PARTICLE NUMBER*)
6 FORMAT(5X,E12.6)
7 FORMAT(5X,*NUMBER OF BACK-SCATTERED PARTICLES=*,I4)
8 FORMAT(6E12.6)
9 FORMAT(5X,*BACK-SCATTERED ENERGY=*,E12.6,5X,*BACK-SCATTERING ANGLE
1=*,F8.4,5X,*BACKSC+AZIMUTHAL ARGLE=*,F8.4/)
11 FORMAT(5X,*NUMBER OF COLLISIONS      *,I3)
12 FORMAT(5X,F8.2)
13 FORMAT(5X,*PROJECTED RANGE - NUMBER/100 ANGSTROMS*)
14 FORMAT(5X,*AVERAGE SCATTERED ENERGY=*,E12.6)
15 FORMAT(5X,*AVERAGE SCATTERED ANGLE=*,F8.4)
16 FORMAT(5X,*DAMAGE ENERGY FRACTION/100 ANG*)
20 FORMAT(5X,E12.6)
21 FORMAT(5X,*DAMAGE ENERGY FRACTION/100 ANG,GT.05 KEV*)
110 FORMAT(3X,F9.5,5X,F7.5,5X,F7.5)
921 FORMAT(6X,*THETA*,9X,*EPS*,8X,*RAND. NO*)
922 FORMAT (5X,I4)
27 FORMAT (5X,I3,4X,2F15.10)
29 FORMAT (5X,*COL NO. DISTANCE      ANGLE*)
```

```
71 FORMAT(5X,4E10.6)
72 FORMAT(5X,3E12.6)
73 FORMAT (5X,*ION HITS A CHANNEL*),
74 FORMAT (5X,E12.6,5X,E12.6)
75 FORMAT (5X,*NUMBER OF CHANNELED PARTICLES=*,I4)

C
91 FORMAT (6X      ,F10.7,5X,F12.4,5X,F12.4)
93 FORMAT (I10)
94 FORMAT (F12.6)
STOP
END

C
C     SUBPROGRAM FN,EP,CN)
FUNCTION FN(X)
COMMON B,CE,CN
X1=(B*EXP(X)-1.)/(B*(EXP(X)-1.))
X2=B*EXP(X)+2./3.
X3=(1.-EXP(-X)/B)**3.
FN=X1*X2*X3*CN
RETURN
END

C
C     SUBPROGRAM FE(EP,CE)
C
C
FUNCTION FE(X)
COMMON B,CE,CN
X1=(B*EXP(X)-1.)/(B*(EXP(X)-1.))
X2=EXP(-X)/B
X3=1.-EXP(-X)/B
FF=X1*X2*X3*CE
RETURN
END

C
C     TOTAL
C
C
FUNCTION FTT(X)
COMMON B,CE,CN
FTT=FN(X)+FE(X)
C
Y=CN   Z=CE
RETURN
END

C
C
SUBROUTINE RUNKUT
4TH ORDER RUNGE-KUTTA METHOD FOR
SOLVING 1 ST ORDER DIFF. EQUATION

C
SUBROUTINE RUNKUT(F,H,X)
REAL K1,K2,K3,K4
CM H=STEP SIZE      X= FT
K1=F(X)
K2=F(X+H*K1/2)
K3=F(X+H*K2/2)
K4=F(X+H*K3)
X=X+H*(K1+2*K2+2*K3+K4)/6.
```

C

C

GLOSSARY

C

C

Z1	ATOMIC NUMBER OF INCIDENT ION
Z2	ATOMIC NUMBER OF THE STRUCK ATOM
A1	ATOMIC WEIGHT OF THE INCIDENT ATOM
A2	ATOMIC WEIGHT OF THE STRUCK ATOM
AD	ATOMIC DENSITY OF CRYSTAL
AV	AVOGADRO'S NUMBER
AMF=MASS OF ELECTRON	
RC	BOHR'S RADIUS
PHIC	CRITICAL ANGLE
EP	TRANSVERSE ENERGY
ET	REDUCED TRANVERSE ENERGY
EO	INITIAL ENERGY OF INCIDENT PARTICLE IN KEV
AT	THOMAS-FERMI SCREENING RADIUS

C

C

C

RETURN

END

6400 END OF RECORD
04.014276628.086000002.014.002.33

0.107000E+08

5.431E+08

100

.239314E+03

.294640E+03

.323965E+03

.343480E+03

.357901E+03

.368395E+03

.376985E+03

.384217E+03

.390437E+03

.395873E+03

.464937E+03

.484499E+03

.494892E+03

.501564E+03

.506285E+03

.509833E+03

.512600E+03

.514850E+03

.516699E+03

.518254E+03

.519581E+03

.520727E+03

.521727E+03

.522608E+03

.523390E+03

.524088E+03

.524716E+03

.525284E+03

.525799E+03

.526269E+03

• 526682E+03
• 527095E+03
• 527459E+03
• 527796E+03
• 528109E+03
• 528399E+03
• 528670E+03
• 528923E+03
• 529160E+03
• 529382E+03
• 948670E-01
• 189734E+00
• 284601E+00
• 379468E+00
• 474335E+00
• 569202E+00
• 664069E+00
• 758936E+00
• 853803E+00
• 948670E+00
• 423854E+01
• 752841E+01
• 108183E+02
• 141081E+02
• 173980E+02
• 206879E+02
• 239777E+02
• 272676E+02
• 305575E+02
• 338474E+02
• 371372E+02
• 404271E+02
• 437170E+02
• 470068E+02
• 502967E+02
• 535866E+02
• 568764E+02
• 601663E+02
• 634562E+02
• 667460E+02
• 700359E+02
• 733258E+02
• 766156E+02
• 799055E+02
• 831954E+02
• 864852E+02
• 897751E+02
• 930650E+02
• 963549E+02
• 996447E+02

END OF FILE

GUSR.
FTN.
LGO.

6400 END OF RECORD
PROGRAM TST (INPUT,OUTPUT,TAPE5=INPUT,TAPE6=OUTPUT)

C
C
C CALCULATION OF CHANNELING LENGTH

C
C MAIN PROGRAM
C

EXTERNAL FE,FN,FT

COMMON B,CE,CN

INTEGER FREQ

555 READ(5,1) A1,A2,Z1,Z2,RHO

READ (5, 2) EI

READ (5,94) RHOAX

READ (5,94) T

READ (5,93) NP

WRITE (6,2) A1

WRITE (6,2) A2

WRITE (6,2) Z1

WRITE (6,2) Z2

WRITE (6,2) RHO

WRITE (6,1) A1,A2,Z1,Z2,RHO

WRITE (6, 2) FI

WRITE (6,94) RHOAX

WRITE (6,94) T

WRITE (6,93) NP

PI=3.14159265

AV=0.62252*1.0E+24

+D=RHO*AV/A2

EK=8.*PI*AD*(4.8*.1E-08)**2*.529*.1E-07/(25.*1.6021*.1E-08)**0.5*

Z1**(.7./6.)*Z2 /(Z1**(.2./3.)+Z2**(.2./3.))**(.3./2.)

Y=SQRT(EI*1.6021*1.E-09)*2.0/EK

WRITE (6,2) EK

WRITE (6,2) Y

ZMAX=Y

FHD=0.0

DO 100 M=1,20

FHD=0.0025+FHD

WRITE (6,2) FHD

G=3.**0.5

Z=(Z1**(.2./3.)+Z2**(.2./3.))**(.3./2.)

AT=0.4685*1.E-08*Z**(-1./3.)

RO=(AD*T*PI)**(1./2.)

EP=EI*FHD**2*1.6021*1.E-09

FT=FP*(T/(Z1*Z2*(4.8*.1E-09)**2))

PHI1=(2.*Z1*Z2*(4.8*0.1E-09)**2/(EI*1.6021*.1E-08*T))**0.5

B=3.*AT**2/(RO**2)+1.0

V=(2.*EI*1.6021*.1E-08/A1)**0.5

PHIC=(G*AT/(2.**0.5*T)*PHI1)**0.5

AME=9.11*1.F-28

VO=2.2*1.0E+08

AO=0.528*1.E-08

ETA=Z1**1./6.

CN1=(PI*AD*T**2)/(EI*1.6021*1.0E-09*G**2*AT**2)

```
CN2=(Z1*Z2*(4.8*.1E-09)**2/T)
CN=CN1*CN2*RHOAX**2
CF1=2.*MAME*AD*T*ETA*PI*AO/(EI*1.6021*1.0E-09*VO)
CE23Z2/Z
CE3=V**3
CF=CF1*CF2*CN2*CF3
EC=G*AT/(2.***1.5*T*PHI1)
WRITE (6,92)
92 FORMAT (*1*,7X,*DEPTH*,11X,*ENERGY TRANS*,3X,* DE/DX*)
```

C
C

```
FREQ=10
DO 114 I=1,NP
W=ZMAX/NP
H=(I-1)*W
WRITE (6,94) ET
CALL RUNKUT(FT,W,ET)
IF (H.GT.Y) GO TO 115
IF (ET.GT.FC) GO TO 200
IF(+.EQ.FREQ)GO TO 31
GO TO 114
31 WRITE (6,91) H,FT,FT(FT)
FREQ=10+FREQ
114 CONTINUE
```

C
C
1 FORMAT(2F10.7,2F4.1,F6.3)
2 FORMAT (5X,F12.6)
93 FORMAT (I10)
94 FORMAT (F12.6)
91 FORMAT (* *,5X,F10.7,5X,F12.4,5X,F12.4)
GO TO 200
115 H=Y
200 WRITE (6,91) H,FT,FT(FT)
100 CONTINUE
STOP
END

C
C
C SUBPROGRAM FN,FP,CN)
FUNCTION FN(X)
COMMON B,CE,CN
X1=(B*EXP(X)-1.)/(B*(EXP(X)-1.))
X2=B*EXP(X)+2./3.
X3=(1.-EXP(-X)/B)**3.
FN=X1*X2*X3*CN
RETURN
END

C
C
C SUBPROGRAM FF(FP,CE)
FUNCTION FF(X)
COMMON B,CE,CN
X1=(B*EXP(X)-1.)/(B*(EXP(X)-1.))
X2=EXP(-X)/B
X3=1.-EXP(-X)/B
FF=X1*X2*X3*CE

RETURN
END

C
C
TOTAL
C

FUNCTION FT(X)
COMMON B,CE,CN
FT=FN(X)+FE(X)
Y=CN Z=CF
RETURN
END

C
C
SUBROUTINE RUNKUT
4TH ORDER RUNGE-KUTTA METHOD FOR
SOLVING 1 ST ORDER DIFF. EQUATION

SUBROUTINE RUNKUT(F,H,X)
REAL K1,K2,K3,K4
H=STEP SIZE X= ET
K1=F(X)
K2=F(X+H*K1/2)
K3=F(X+H*K2/2)
K4=F(X+H*K3)
X=X+H*(K1+2*K2+2*K3+K4)/6.

C
C
GLOSSARY

Z1 ATOMIC NUMBER OF INCIDENT ION
Z2 ATOMIC NUMBER OF THE STRUCK ATOM
A1 ATOMIC WEIGHT OF THE INCIDENT ATOM
A2 ATOMIC WEIGHT OF THE STRUCK ATOM
AD ATOMIC DENSITY OF CRYSTAL
AV AVOGADRO'S NUMBER
AME=MASS OF ELECTRON
VO BOHR'S RADIUS
PHIC CRITICAL ANGLE
EP TRANSVERSE ENERGY
ET REDUCED TRANSVERSE ENERGY
EO INITIAL ENERGY OF INCIDENT PARTICLE IN KEV
AT THOMAS-FERMI SCREENING RADIUS

C
C
C
RETURN
END

6400 END OF RECORD

01.014276628.086000001.014.002.33

1.2

0.107000E-08

5.431E-08

100

END OF FILE
END OF FILE

REFERENCES

- [1] J. Lindhard and M. Scharff, Phys. Rev. 124, 128 (1961).
- [2] J. Lindhard, M. Scharff and H.E. Schiøtt, Mat. Fys. Medd. Dan. Vid. Selsk. 33,14 (1963).
- [3] K.B. Winterbon, P. Sigmund and J.B. Sanders, Mat. Fys. Medd. Dan. Vid. Selsk. 37,14 (1970).
- [4] J. Lindhard, Mat. Fys. Medd. Dan. Vid. Selsk. 34, 14 (1965).
- [5] D.V. Morgan, 'Channeling', John Wiley & Sons, 1973.
- [6] J.E. Robinson, Rad. Effects 00, (1974).
- [7] S. Agamy, M.Eng. Thesis, McMaster Univ., 1973
- [8] J.H. Barrett, Phys. Rev. B, Vol. 3, 5 (1971)